

RESEARCH ARTICLE

Hepatocyte nuclear factor 4 α negatively regulates connective tissue growth factor during liver regeneration

Junmei Zhou^{1,2} | Xiaowei Sun^{1,3} | Lu Yang⁴ | Liquan Wang⁵ | Gai Ran^{1,6} | Jinhui Wang⁴ | Qi Cao⁷ | Lizi Wu⁸ | Andrew Bryant⁵ | Chen Ling^{1,6} | Liya Pi¹

¹Department of Pediatrics, University of Florida, Gainesville, FL, USA

²Institute of Cardiovascular Disease, Key Laboratory for Arteriosclerosis of Hunan Province, University of South China, Hengyang, China

³Institute of Pathology, School of Basic Medical Sciences, Lanzhou University, Lanzhou, China

⁴Integrative Genomics Core, Beckman Research Institute of the City of Hope, Duarte, CA, USA

⁵Department of Medicine, University of Florida, Gainesville, FL, USA

⁶State Key Laboratory of Genetic Engineering, School of Life Sciences, Zhongshan Hospital, Fudan University, Shanghai, China

⁷Department of Diagnostic Radiology and Nuclear Medicine, University of Maryland School of Medicine, Baltimore, MD, USA

⁸Department of Microbiology & Molecular Genetics, College of Medicine, University of Florida, Gainesville, FL, USA

Correspondence

Chen Ling, State Key Laboratory of Genetic Engineering, School of Life Sciences, Zhongshan Hospital, Fudan University, Shanghai 200438, China.
Email: lingchenchina@fudan.edu.cn

Liya Pi, Department of Pediatrics, University of Florida College of Medicine, 1200 S Newell Drive, Gainesville, FL 32610, USA.
Email: lpi@peds.ufl.edu

Funding information

HHS | NIH | National Institute on Alcohol Abuse and Alcoholism (NIAAA), Grant/Award Number: KO1AA024174 and R01AA028035; Children Miracle Network Foundation; National Key Research and Development Program of China, Grant/Award Number: 2018YFA0109400; Shanghai Sailing Program, Grant/Award Number: 17YF1401300; Shanghai Eastern Scholarship, Grant/Award Number: TP2016004

Abstract

Liver regeneration after injury requires fine-tune regulation of connective tissue growth factor (Ctgf). It also involves dynamic expression of hepatocyte nuclear factor (Hnf)4 α , Yes-associated protein (Yap), and transforming growth factor (Tgf)- β . The upstream inducers of Ctgf, such as Yap, etc, are well-known. However, the negative regulator of Ctgf remains unclear. Here, we investigated the Hnf4 α regulation of *Ctgf* post-various types of liver injury. Both wild-type animals and animals contained siRNA-mediated *Hnf4 α* knockdown and Cre-mediated *Ctgf* conditional deletion were used. We observed that *Ctgf* induction was associated with Hnf4 α decline, nuclear Yap accumulation, and Tgf- β upregulation during early stage of liver regeneration. The *Ctgf* promoter contained an Hnf4 α binding sequence that overlapped with the *cis*-regulatory element for Yap and Tgf- β . *Ctgf* loss attenuated inflammation, hepatocyte proliferation, and collagen synthesis, whereas *Hnf4 α* knockdown enhanced *Ctgf* induction and liver fibrogenesis. These findings provided a new mechanism about fine-tuned regulation of *Ctgf* through Hnf4 α antagonism of Yap and Tgf- β activities to balance regenerative and fibrotic signals.

KEY WORDS

connective tissue growth factor (Ctgf), hepatocyte nuclear factor 4 α (Hnf4 α), liver injury, liver regeneration

Abbreviations: α SMA, α smooth muscle actin; CCl₄, carbon tetrachloride; ChIP, chromatin immunoprecipitation; CD, cluster of differentiation; Ctgf, connective tissue growth factor; DNA, deoxyribonucleic acid; DR, direct repeat; GS, glutamine synthetase; HCC, hepatocellular carcinoma; Hnf4 α , hepatocyte nuclear factor 4 α ; IHC, immunohistochemistry; IL1 α , interleukin 1 α ; mRNA, messenger ribonucleic acid; PH, partial hepatectomy; PCR, polymerase chain reaction; SEAP, secreted alkaline phosphatase; siRNA, small interfering ribonucleic acid; TEAD, transcriptional enhanced associate domain; Tgf- β , transforming growth factor- β ; Tnf α , tumor necrosis factor α ; Yap, yes-associated protein.

Junmei Zhou and Xiaowei Sun are contributed equally to this work.

This is an open access article under the terms of the Creative Commons Attribution-NonCommercial License, which permits use, distribution and reproduction in any medium, provided the original work is properly cited and is not used for commercial purposes.

© 2020 The Authors. The FASEB Journal published by Wiley Periodicals LLC on behalf of Federation of American Societies for Experimental Biology.

1 | INTRODUCTION

The liver is a critical metabolic and digestive organ. It exposes to exogenous and endogenous toxins daily, such as alcohol, viruses, etc. In addition, drug-induced liver injury is a leading cause of death worldwide and complicates various drug treatment.¹ Fortunately, the liver possesses an extraordinary ability to regenerate. Liver regeneration is a process of compensatory hyperplasia with hepatocyte replication to restore parenchymal loss.² During regeneration, immune cells are rapidly recruited. They induce hepatocyte priming before cell cycle re-entry, followed by waves of proliferation of parenchymal and nonparenchymal cells. At the end of liver regeneration, extracellular matrix is synthesized and deposited onto new tissues. These regenerative processes go awry in chronic liver diseases. Persistent insults cause chronic inflammation, severe hepatocyte damage, and sustained activation of myofibroblast cells. These cells produce excessive amounts of collagen leading to liver fibrosis. If left untreated, cirrhosis and liver cancer may eventually develop.³ To date, no reliable cue for fibrosis exists. Understanding molecular mechanism governing liver regeneration and liver fibrosis is pre-requisite for many therapeutic interventions that optimize regenerative outcome and avoid scar formation after liver injury.

Increased cell plasticity is a key feature in liver regeneration. For instances, hepatocytes downregulate the epithelial genes and undergo epithelial to mesenchymal transition after partial hepatectomy (PH).⁴ Cross-regulatory cascades driven by hepatocyte nuclear factor (Hnf4 α) and the Hippo/Yes associated protein (Yap) pathway have been shown to control hepatocyte differentiation and dedifferentiation. Hnf4 α globally maintains the hepatocyte differentiation and function via binding to promoter sequences of thousands of genes. Loss of Hnf4 α has been found after liver injury or during hepatocellular carcinoma (HCC) development. Re-activation of this transcriptional factor is essential for termination of liver regeneration.⁵ In contrast, Yap is ordinarily inactive in cytoplasm via phosphorylation by the Hippo kinases that maintain quiescence in the liver.⁶ During liver injury, Yap is activated so that its nonphosphorylated form enters nuclei and binds to members of transcriptional enhanced associate domain (TEAD) family to turn on target genes. Connective tissue growth factor (Ctgf) of the Cyr61/CTGF/Nov protein family is a known Yap target. It promotes HCC through autocrine action.^{7,8} Ctgf protein is also profibrotic. It binds to transforming growth factor (Tgf)- β , leading to enhanced Tgf- β /Smad3 signaling.^{9,10} Overexpression of *Ctgf* in hepatocytes renders liver susceptibility to fibrogenesis stimuli.¹¹ Although *Ctgf* upregulation after liver injury has been reported in experimental and human studies,^{9,12,13} its fine-tune regulation during liver regeneration still remains elusive. In this paper, we utilized multiple mouse models of liver regeneration and

demonstrated Hnf4 α antagonism of Yap activities via a novel *cis*-regulatory element in the *Ctgf* promoter.

2 | MATERIALS AND METHODS

2.1 | Generation of *Ctgf* conditional knockouts

All animal protocols were approved by the University of Florida Animal Care and Usage Committee and were conducted in compliance with their guidelines. *Ctgf* conditional knockouts (*Ctgf*^{ko/ko}) were previously published.^{14,15} These mice carried two loxP sites flanking exon 4 of *Ctgf* (termed *Ctgf*^f) gene and one allele of the human ubiquitin C promoter (*ubc*)-*Cre/ERT2* transgene. At 3-week-old age, *Ctgf*^{ff} mice carrying *ubc-Cre/ERT2* were given IP injection of the tamoxifen suspension (75 mg/kg body weight) over 5 days and the resulting *Ctgf*^{ko/ko} mice lost exon 4 of *Ctgf* in genotyping analysis using primers and PCR condition described previously.¹⁶ One month later, these mice were fed with the Lieber-DeCarli liquid diet (BioServ, Flemington, NJ) containing 1% ethanol for 2 days followed by 2% ethanol for 10 days. Carbon tetrachloride (CCl₄, 1 μ L/g body weight) was injected through IP at 1 day before the end of experiment.

2.2 | Hepatocyte damage to induce liver regeneration following PH or CCl₄ intoxication in combination with or without moderate ethanol exposure

For surgical resection, wild-type mice (n = 35) were subjected to PH by excision of the median and left lateral liver lobes at their stem under aseptic conditions according to previous publication.¹⁷

For CCl₄ intoxication in combination with or without ethanol feeding, wild-type or mutant mice (8-10 week old) were subjected to moderate ethanol feeding using the Lieber-DeCarli liquid diet (BioServ, Flemington, NJ) containing 1% ethanol for 2 days followed by 2% ethanol for the duration of the experiment based on previous publication.¹⁸ Isocaloric maltose was administered to a pair-fed cohort. After that, 2% ethanol was fed for the remaining experiments. An average of 13.1 mL of the 2% ethanol-containing diet was consumed per day. Pair-fed mice were given an isocaloric diet in which ethanol calories were substituted with calories from maltose dextrin. Pair-fed animals received a diet volume equivalent to that of their ethanol-fed experimental counterparts on the previous day to ensure equivalent calories were consumed between groups. No differences were seen in final body weight between pair and ethanol-fed mice at any experimental time point. Ethanol-fed (n = 35) or pair-fed (n = 35) mice received a

single acute dose of CCl_4 (1 $\mu\text{L/g}$ body weight) prediluted 1:3 in olive oil and administered via intraperitoneal (IP) injection.

2.3 | Knockdown of *Hnf4a* and generation of piLenti-si*Hnf4a* viral vectors

For knockdown in human *HNF4a* gene in HepG2 cells, Stealth siRNA containing 25 bp double-stranded RNA oligonucleotides were obtained (ThermoFisher, Carlsbad, CA). The target sequence is 5' CCAGUAUGACUCGCGUGGCCGCUU 3' that corresponds to 1017-1041 bp of this gene (GenBank: BC137539.1). The *HNF4a* siRNA and Stealth RNAi negative control duplexes (50 nM) were transfected into cells with Lipofectamine RNAiMAX transfection reagent (ThermoFisher). Two days later, cells were lysed for RNA and protein isolation. *HNF4a* transcript was amplified using primer pair 5' CACGGGCAAACACTACGGT 3' (sense) and 5' TTGACCTTCGAGTGCTGATCC 3' (antisense) with standard conditions in RT-PCR analysis.

To knock down mouse *Hnf4a* gene, we obtained plasmids corresponding to piLenti-GFP scramble siRNA and piLenti-GFP si*Hnf4a* #1-4 from Applied Biological Materials Inc., BC, Canada (Abm). The siRNA#1-4 contained 29-bp sequences targeting open reading frame of mouse *Hnf4a* gene (NM_008261.2) starting at 298, 562, 833, and 1124 bp, respectively. Mouse hepatoma Hepa1-6 cells (ATCC, Gaithersburg, MD) were grown in Dulbecco's Modified Eagle's Medium (DMEM) supplemented with 10% fetal bovine serum (FBS) and transfected with piLenti-GFP si*Hnf4a* plasmids. Two days later, messenger RNAs (mRNAs) and proteins were extracted and analyzed by RT-PCR and Western blotting to determine their effects on *Hnf4a* inhibition. Relative *Hnf4a* was normalized against reference gene (*18S*) and calculated in delta delta CT methods from triplicate tests in relation to scramble.

High-titer viruses for piLenti-GFP si*Hnf4a*#3 and piLenti-GFP scramble siRNA were produced after cotransfection of lentiviral backbone as well as packaging plasmids that contain constructs encoding Gag/Pol, Rev, VSVG genes, respectively in 293T cells according to the manufacturer's instruction (Applied Biological Materials Inc). The transfection efficiency was evaluated 24 hours post-transfection by the percentage of positive GFP cells observed under a fluorescence microscope. Two days after transfection, the culture supernatant was collected, filtered via 0.45- μm filter and concentrated through ultracentrifugation according to previous publication.¹⁹ Lentiviral particles at 1.0×10^{10} infectious unit (IU)/mL were delivered via tail vein injection into wild-type C57BL6/J mice. After the lentiviral injection, animals were subjected to moderate ethanol feeding using the Lieber-DeCarli liquid diet containing 1%-2% ethanol for as described above. Ten days later, a single acute dose of CCl_4

(1 $\mu\text{L/g}$ body weight) was given. Livers were harvested 2 days after the chemical-induced liver injury.

2.4 | RNA isolation, RT-PCR, qRT-PCR, and RNA sequencing analysis

Total RNAs were extracted using RNeasy Mini kit (Qiagen, Valencia, CA). Total RNA isolation and cDNA synthesis were reported previously.²⁰ In brief, total RNA was incubated with RQ1 RNase-free DNase (Promega, Madison, WI) to remove genomic DNA. Template cDNA was synthesized using reverse transcriptase in Superscript III First-Strand Synthesis with 50 pmol random hexamer (Invitrogen). RT-PCR analysis was carried out using 0.5 μL of cDNAs templates, 0.2 μM of each set of primers (listed in Supplementary Table 1), and 1 \times REExtract-N-Amp tissue PCR kit (Sigma, St. Louis, MO) with standard amplification conditions that consisted of thirty cycles of denaturation at 94°C for 30 seconds, annealing at 55°C for 30 seconds, and extension at 72°C for 30 seconds. The quantitative RT-PCR (qRT-PCR) analysis for *Ctgf* was carried out using SYBR Green PCR master mixer (Applied Biosystems, Foster City, CA) with the following primer set *Ctgf*: 5' AGTGGAGCGCTGTTCTAAG 3' (sense) and 5' GTCTTCACACTGGTGACAGCC 3' (antisense). These primers detected exon 4 deletion in *Ctgf* deficient livers. Amplified products were analyzed in ABI Prism 7900 HT Fast Real-Time (Applied Biosystems). All qRT-PCR experiments were performed in triplicate using cDNA sample from independent RNA sets and the relative amount of target mRNA was calculated using delta-delta CT method and normalized against reference gene (*18S*) in each sample.

For RNA-sequencing, total RNAs were isolated from ethanol/ CCl_4 -treated livers of *Ctgf*^{+/k}, *Ctgf*^{+/f}, *Yap1* KO, and *Yap1*^{fllox/fllox} using RNeasy Extraction Kit from Qiagen. RNA-sequencing was carried out using an Illumina HiSeq 2500 system following manufacturer's protocols (Illumina Inc. San Diego, CA). In brief, cDNA synthesis and fragmentation were carried out with the 200 bp peak setting by Covaris S220 (Covaris Inc., Woburn, Massachusetts). End repair, 3' end adenylation and the barcoded adapters (Illumina) were performed to the fragmented cDNA in prior to ligation with Kapa LT library preparation kit (Kapa Biosystems, Wilmington, MA). The prepared libraries were validated using a 2100 Bioanalyzer DNA High Sensitivity chip, and quantified by Qubit Fluorometric Quantitation (Waltham, MA). The library templates were prepared for the sequencing using cBot cluster generation system with HiSeq SR Cluster Kit V4 (Illumina). The sequencing run was performed in a single read mode of 51 cycles of read 1 and 7 cycles of index read using HiSeq 2500 platform with HiSeq SBS Kit V4 (Illumina). HiSeq Control Software (HCS) 2.2.38 and Real Time Analysis (RTA) 1.18.61 on the

Illumina HiSeq 2500 machine were used for image analysis and base calling. Raw sequence reads were mapped to the mouse genome using STAR,²¹ and the frequency of Refseq genes was counted using HTseq.²² The raw counts were then normalized using the trimmed mean of M values (TMM) method and compared using Bioconductor package “edgeR”.²³ Reads per kilobase per million (RPKM) mapped reads were also calculated from the raw counts. Differentially expressed genes were identified if RPKM ≥ 1 in at least one sample, fold change ≥ 2 , and $P \leq .05$. These differential genes were then imported into DAVID for GO category enrichment analysis.²⁴

2.5 | Histology and morphometry

Blood samples and liver tissue were collected under deep anesthesia. Trimmed liver tissues were fixed in 4% paraformaldehyde PBS solution. Histology and immunofluorescent staining were performed with standard protocols using the antibodies, dilutions, and retrieval conditions listed in Supplementary Table 2. In brief, 5 μm formalin fixed paraffin embedded sections were rehydrated, blocked with 3% H_2O_2 in methanol for 10 minutes, subjected to the required retrieval conditions and then sequentially blocked in avidin and biotin solutions for 15 minutes each. Primary antibodies for Yap, Hnf4 α , and Ki67 were applied overnight at 4°C. Detection was carried out according to the manufacturer’s instructions using the ABC-Elite kit with ImmPACT DAB substrate (Vector Laboratories, Burlingame, CA). In addition, immunohistochemistry (IHC) for either Ctgf or CD11b in liver sections was detected using a VECTASTAIN ABC-AP kit and Vector Alkaline Phosphatase Red substrate (Vector Laboratories). The immunofluorescence staining for glutamine synthetase (GS) was carried out using the rabbit antibody listed in Supplementary Table 2. Alexa Fluor 488 or 594 conjugated donkey anti-rabbit secondary antibody (Invitrogen, Carlsbad, CA) were used for detection. For an estimation of percent necrosis, paraffin-embedded liver sections were subjected to standard H&E staining. Images were captured with CellSens software using an Olympus BX 51 upright fluorescence microscope outfitted with an Olympus DP80 camera, Plan Fluorite objectives and an LED transmitted light source (Olympus). DAB stained areas were quantified from 10 random fields of images (200 \times magnification) using Image J software (<http://rsb.info.nih.gov/ij/>) and IHC profiler according to published methods.²⁵

2.6 | PCR-based ChIP assays

PCR-Based ChIP assays were performed in HEK293 cells using the SimpleChIP Plus Enzymatic Chromatin IP kit

(Cell Signaling Inc, Danvers, MA) according to the manufacturer’s instructions. In brief, HEK293 cells carrying Myc-DDK fused Yap, Smad3, or Hnf4 α were cross-linked with formaldehyde, neutralized in glycine, digested by micrococcal nuclease, and then sonicated. The resulting chromatin was pre-cleared with Protein A conjugated magnetic beads followed by incubating with magnetic beads and five micrograms of specific or control antibody overnight. Specific antibodies are anti-Yap (Cell Signaling), anti-Smad3 and anti-Hnf4 α (Santa Cruz Technologies, Dallas, TX). The beads were then washed, and the chromatin was eluted in ChIP elution buffer, reverse-cross-linked at 65°C overnight, and treated with RNase and Proteinase K. The DNA was extracted, and 2 μL of DNA was used for each ChIP-qPCR experiment. Quantitative real time PCR was performed using SYBR Green PCR master mix (Applied Biosystems) according to standard amplification conditions with the following primer sets: for Yap, Smad3 or Hnf4 α binding: 5’ ATATGAATCAGGAGTGGTGCGA 3’ (sense) and 5’ CAACTCACACCGGATTGATCC 3’ (antisense). The percentage of input was calculated using the Ct value of the input DNA and ChIP-DNA. The data were normalized to the value of the IgG control antibody.

2.7 | Western blotting and ELISA assays

Western blotting was performed as previously described,²⁶ with modification. Total proteins were extracted from mouse livers or cultured cells in RIPA buffer containing complete Proteinase Inhibitor (Sigma). Nuclear fractions were isolated using NE-PER Nuclear and Cytoplasmic Extraction Reagents (ThermoFisher Scientific). Nuclear fractions (10 μg) or total protein lysates (50 μg) were boiled in 1 \times Laemmli buffer containing 5% β -mercaptoethanol, separated on 4%-12% Bis-Tris protein gels (Novex, Carlsbad, CA), and electro-transferred onto polyvinylidene difluoride (PVDF) membrane for immunoblotting. Primary antibodies used were mouse anti-Smad3 (Santa Cruz Technologies), rabbit anti-Yap (Cell Signaling), rabbit anti-Hnf4 α (Santa Cruz Technologies), mouse anti-Cyclin D1 (Santa Cruz Technologies), mouse anti-Actin (Abcam, Cambridge, MA), mouse anti-Myc (Thermo Scientific), rabbit anti-Ctgf (Abcam), rabbit anti-collagen type I (Abcam), and rabbit anti-GAPDH (Abcam). Detection was carried out using horseradish peroxidase-conjugated secondary antibodies (Santa Cruz biotechnologies) and the ECL Plus kit (Amersham Biosciences, Piscataway, NJ).

Serum levels of Tnf α and IL1 α were determined from liver samples using ELISA kits (R&D systems, Minneapolis, MN, USA) according to the manufacturer’s instructions. Absorbance at wavelength of 450 nm was measured using the Titertek Multiskan Plus MKII microplate reader.

2.8 | Cell lines

HEK293 and HepG2 cells were cultured in DMEM supplemented with 10% FBS, 100 mg of penicillin/ml, and 100U of streptomycin/ml. AML12 mouse hepatocytes were from ATCC Inc and cultured in DMEM/F12 media containing 10% FBS, 400 nM dexamethasone, 1x insulin, transferrin, and selenium (ITS). LX-2 human stellate cells were from Dr. Scott Friedman (Mount Sinai School of Medicine, New York) and cultured in DMEM with 2% FBS. All cells were maintained in a humidified 37°C incubator with 5% CO₂.

2.9 | Secreted alkaline phosphatase assay

A reporter plasmid carrying secreted alkaline phosphatase (SEAP) under the control of human *CTGF* promoter was a kind gift from Dr. Andrew Leask (Western University, Canada). Plasmids carrying Myc-DDK tagged cDNAs for murine Yap (GeneBank accession# NM_001171147), and Hnf4 α (NM_008261) were purchased (OriGene, Rockville, MD). These plasmids, empty pCMV6 vector or in combination (100 ng per well) were transfected into HEK293 or HepG2 cells in 24-well plates. To knockdown human Hnf4 α , 50 nM Stealth RNA oligonucleotides or non-targeting scramble control was also transfected. One day after transfection, media were switched to conditioned media containing with or without Tgf- β 1 (5 ng/mL). A pCMV-lacZ plasmid (Clontech) at 20 ng/well was transfected as internal control for normalization based on β -galactosidase activities in the co-transfected cells according to Leask et al.²⁷ The SEAP activity was measured in conditioned medium 48 hours later using the Great EscAPE SEAP Chemiluminescence kit (Clontech, Mountain View, CA) according to the manufacturer's instructions. SEAP activities were measured in triplicate experiments and relative *CTGF* promoter activity was expressed as fold change in comparison to the normalized SEAP activities of vector controls.

2.10 | EMSA and site directed DNA mutagenesis in *CTGF* promoter

The following primers were biotinylated using Pierce Biotin 3' End DNA labeling kit (ThermoFisher Scientific) for EMSA. 5' ATGCTGAGTGTCAAGGGGTCAGGATCAA 3' (sense) and 5' TTGATCCTGACCCCTTGACACTCAGCAT 3' (antisense) were for wild-type human *CTGF* probes. 5' CAGACGGAGGAATGCTGATTTTCTTTTTTTCAGGATCAATCCGGTGT 3' (sense) and 5' ACACCGGATTGATCTGAAAAAAGAAAATCAGCATTCCTCCGTCTG

3' (antisense) were for the mutant human *CTGF* probe. A mobility shift reaction mixture was set up using LightShift Chemiluminescent EMSA kit (ThermoFisher Scientific). It contained crude nuclear extracts overexpressing Hnf4 α :Myc or Yap:Myc proteins (2 mg), poly(dIdC) (1mg), 0.1 mg of sonicated denatured salmon sperm DNA, biotin-labeled wild-type or mutant probe (4 pmol). Cold probe (20 fmol) was added in some experiments to determine binding specificities of tested probes. Antibodies against Hnf4 α and Myc epitope (1 μ g) were also included in some reactions for super-shift assays. Complexes in reaction mixtures (20 μ L) were separated in polyacrylamide gel and electro-transferred onto a nylon membrane for immunoblotting. The biotin end-labeled DNA probe was detected using streptavidin conjugated to horseradish peroxidase and chemiluminescent substrate according to manufacturer's instructions in the EMSA kit.

For site directed DNA mutagenesis, a strategy was designed to replace "5' GTCAAGGGGTCAGG 3'" in the putative HNF4 α binding site of the human *CTGF* promoter with mutant sequences "5' TTAAACAACTAGT 3'" using two sets of complementary primers: P1151 primer: 5' ACGGAGGAATGCTGAGTTTAAACAA actagtATCAATCCGGTGTGAGTT 3'; P1152 primer: 5' AACTCACACCGGATTGATactagtTTGTTTAAACTCAGCATTCCCTCCGT 3'; P1153 primer: 5' TAACTGGCTTCAGCAGAGCGCAGATACCAAATACTGTCCTTCTA 3', and P1154 primer: 5' TAGAAGGACAGTATTTGGTATCTGC GCTCTGCTGAAGCCAGTTA 3'. SpeI restriction enzyme site (underlined and lowercase) was introduced in the mutant *CTGFp* to facilitate verification of mutations after cloning. P1151 and P1153 primer pairs were used to generate a 3538 bp PCR product containing sequences for the mutated *CTGF* promoter driven SEAP using the Gibson Assembly Site Directed Mutagenesis kit (SGI-DNA). P1152 and P1154 primer pairs were also used to amplify a 2000 bp PCR product that corresponded to the rest sequences of the SEAP reporter using the same kit. *KpnI* and *XhoI* restriction enzyme sites at the 5' and 3' ends of the human *CTGF* promoter were designed for cloning to re-assemble a full SEAP reporter with the correct orientation that carried mutations in the putative HNF4 α binding site. The resulting plasmid with mutations was transformed into NEB 5 alpha competent cells (New England Biolabs, Ipswich, MH). Mutations were verified by SpeI digestion and sequencing analysis.

2.11 | Statistical analysis

GraphPad Prism 6.0 (GraphPad Software) was used for statistical analysis. Statistical significance ($P < .05$ -.0005) was evaluated using the Student's *t* test and one-way analysis of variance (ANOVA).

3 | RESULTS

3.1 | *Ctgf* deficiency attenuates liver regeneration after ethanol/CCl₄-induced injury

Moderate ethanol feeding has been shown to aggravate hepatocyte damage, potentiate hepatocyte proliferation, and enhance liver fibrogenesis after acute CCl₄ intoxication.²⁸ Indeed, ethanol/CCl₄ co-treatment caused slower resolution of necrotic liver mass (Supplementary Figure 1A). This slower removal of hepatic necrosis paralleled greater ratios between liver and body weights at 24-96 hours post the chemical induced injury in ethanol-fed groups than paired groups (Supplementary Figure 1B). Compared to single treatment with CCl₄ alone, more fibrogenesis occurred after ethanol/CCl₄ co-treatment as evidenced by increased expression of α smooth muscle actin (α SMA), and collagen type I (Supplementary Figure 1C). Higher levels of Cyclin D1, Tgf- β 1, and most importantly, *Ctgf*, were also observed after ethanol/CCl₄ co-treatment (Supplementary Figure 1D).

In order to determine the function of *Ctgf* during liver injury after ethanol/CCl₄ co-treatment, we deleted this gene utilizing *Ctgf*^{*fl/fl*} carrying *ubc-Cre/ERT2* that mediated exon4-deletion in a tamoxifen-inducible manners.¹⁴ Liver tissues were obtained from ethanol-fed *Ctgf*^{*fl/fl*} mice and their

Ctgf^{*fl/fl*} littermates at 24 hours after CCl₄ administration. Loss of *Ctgf* gene products was confirmed by RT-PCR (Figure 1A), Western blotting (Figure 1B) and IHC staining (Figure 1C). It was evident that injury-induced *Ctgf* expression was limited to periportal areas in *Ctgf*^{*fl/fl*} livers, whereas minimal *Ctgf* expression was detected in *Ctgf*^{*fl/fl*} livers (Figure 1C). RNA Seq was further carried out to identify differentially expressed genes and pathways between the damaged *Ctgf*^{*fl/fl*} and *Ctgf*^{*fl/fl*} livers. *Ctgf* deletion caused downregulation of genes in inflammatory cytokines, positive regulation of cell proliferation, and collagen fibril organization downstream of MAPK and PI3K-Akt signaling pathways from functional enrichment analysis (Table 1). In addition, decreased protein expressions of Cyclin D1 and collagen type I (Figure 1B) as well as reduced mRNA levels of *Ccnd1*, *Col5a2*, *Col1a1*, and *Col1a2* (Supplementary Figure 2) were confirmed upon *Ctgf* deletion. Furthermore, tumor necrosis factor (*Tnfa*) and *IL1 α* in the damaged *Ctgf*^{*fl/fl*} livers were lower at both mRNA and protein levels in comparison to those of *Ctgf*^{*fl/fl*} controls (Figure 1D,E). This attenuated inflammation was associated with reduced recruitment of cluster of differentiation (CD)11b⁺ cells (Figure 1F, upper). Concomitant decrease of hepatocyte proliferation was also evidenced by reduced number of proliferating hepatocytes in Ki67 staining (Figure 1F, lower). These observations indicated that *Ctgf* deficiency

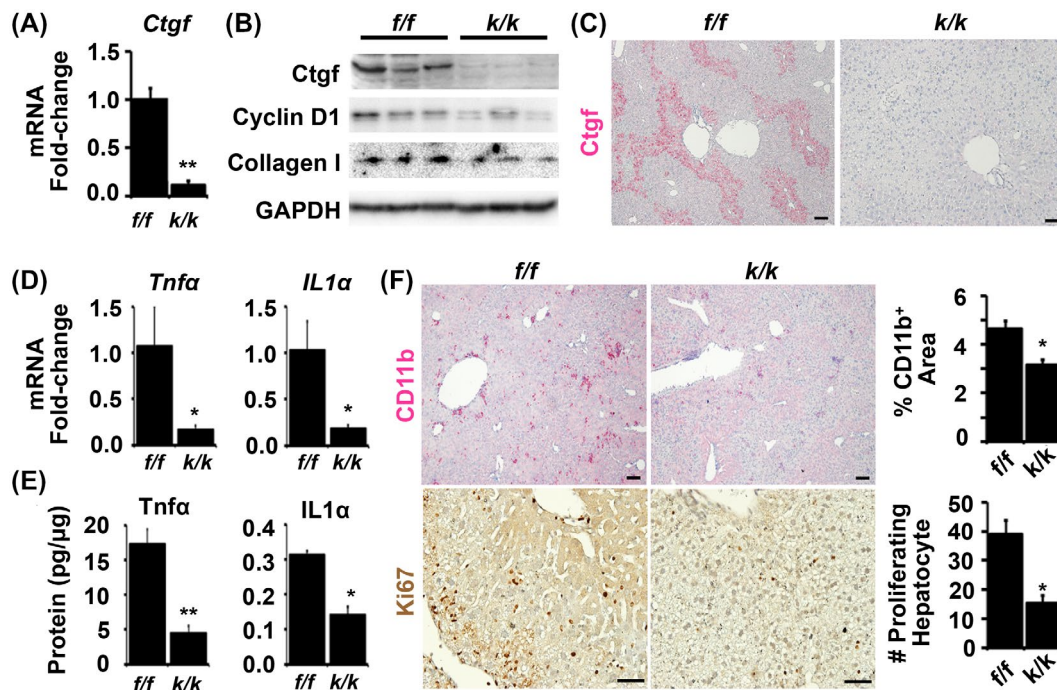


FIGURE 1 *Ctgf* deficiency is associated with reduced inflammation, hepatocyte proliferation, and collagen production after liver damage caused by ethanol/CCl₄ co-treatment. *Ctgf*^{*fl/fl*} and *Ctgf*^{*fl/fl*} mice were subjected to ethanol/CCl₄ co-treatment and were sacrificed at day 1 after CCl₄ administration. (A-C) *Ctgf* loss was confirmed by qRT-PCR analysis (A), Western blotting (B) and IHC staining (C). Downregulated *Tnfa* and *IL1 α* expression in the damaged *Ctgf*^{*fl/fl*} livers were examined by qRT-PCR analysis (D) and ELISA assays (E). (F) IHC staining showed that *Ctgf* deficiency reduced recruitment of CD11b⁺ macrophages and number of Ki67⁺ proliferating hepatocytes. Scale bar: 10 μ m. Quantification was calculated from 10 random fields at 200 \times magnification based on staining of three different livers per group. Data are means \pm SD (n = 3 per group). **P* < .05 and ***P* < .005 (Student's *t*-test)

TABLE 1 Functional enrichment analysis identifies genes and pathways that are reduced in *Ctgf* conditional knockouts after ethanol/ CCl_4 -induced liver injury

Term	Fold enrichment	P value	Genes
GO:0006954~inflammatory response	7.3005490	7.76E-06	<i>Tnf, IL1a, Csf1r, Ifi202b, Nfkbiz, P2rx7ln, Anxa1, Tnfaip3, Nlrp3</i>
GO:0008284~positive regulation of cell proliferation	4.1702029	0.001	<i>Ccnd1, Tnf, Enpp2, Jun, Camp, Ntrk2, Zfp703, Sox4, CSF1R</i>
GO:0030199~collagen fibril organization	25.757834	4.79E-04	<i>Col1a2, Col1a1, Lox, Col5a2</i>
mmu04010:MAPK signaling pathway	5.384794234	0.004	<i>Tnf, Jun, Ntrk2, Dusp10, Dusp8, IL1a</i>
mmu04151:PI3K-Akt signaling pathway	3.881347411	0.016	<i>Ccnd1, Itgb7, Col1a2, Col1a1, Col5a2, Csf1r</i>

Abbreviations: Anxa1: annexin A1; Camp: cathelicidin antimicrobial peptide; Ccnd1: cyclin D1; CSF1R: colony-stimulating factor 1 receptor; Col1a2: collagen, type I alpha-2; Col1a1: collagen, type I alpha-1; Col5a2: collagen, type V alpha-2; Dusp10: dual specificity phosphatase 10; Dusp8: dual specificity phosphatase 8; Enpp2: ectonucleotide pyrophosphatase/phosphodiesterase 2; Ifi202b: interferon activated gene 202B; IL1alpha: interleukin 1 α ; Itgb7: integrin beta-7; Jun: v-Jun avian sarcoma virus 17 oncogene homolog; Lox: lysyl oxidase; Lxn: Latexin; Nlrp3: NLR family, pyrin domain-containing 3; Nfkbiz: nuclear factor of kappa light chain gene enhancer in b cells inhibitor, zeta; Ntrk2: neurotrophic tyrosine kinase, receptor; P2rx7: purinergic receptor p2x, ligand-gated ion channel, 7; Sox4: Sry-box 4; Tnf: tumor necrosis factor alpha; Tnfaip3: tumor necrosis factor alpha-induced protein3; Zfp703: zinc finger protein 703.

attenuated hepatic inflammation, hepatocyte proliferation, and collagen production during liver regeneration after ethanol/ CCl_4 -induced injury.

3.2 | Hnf4 α expression is negatively correlated to *Ctgf* expression after liver injury

Hepatocyte nuclear factor (Hnf)4 α , Yap, and Smad3 of the Tgf- β 1 signal transduction pathway are all necessary for liver regeneration after injury. Thus, we compared their expression patterns following ethanol/ CCl_4 co-treatment. As shown in Figure 2A, hepatocytes re-entered cell cycle as indicated by increased amounts of Cyclin D1 post-injury. Yap and Smad3 were upregulated from 2 to 72 hours after the chemical induced injury. Coincidentally, *Ctgf* protein was rapidly upregulated within the first 4 hours post-treatment and reduced to a basal level at 72 hours. In contrast, Hnf4 α was decreased at 2-24 hours post the injury. The inductions of Yap and *Ctgf* proteins as well as loss of Hnf4 α protein were further confirmed by IHC and immunofluorescence staining (Figure 2B). Interestingly, dual staining labeled *Ctgf* and Hnf4 α proteins in the same populations of periportal hepatocytes (Figure 2C,D), implicating a potential regulation between *Ctgf* and Hnf4 α expression. Similar results were observed during liver regeneration that was induced by CCl_4 alone (Supplementary Figure 3A-C).

Another commonly used model of liver regeneration is PH. As shown in Figure 3A,B, *Ctgf* mRNA and protein were rapidly upregulated within the first 3 hours after PH while *Tgf- β 1* was induced up to 24 hours before the peak of hepatocyte proliferation as indicated by induction of *Ccnd1* mRNA and protein at 24-72 hours post injury. These changes were correlated with transient decline of Hnf4 α at the first half hour post PH, and nuclear localization of Yap and Smad3

proteins at 0.5-24 hours after PH (Figure 3C,D). IHC staining showed that Hnf4 α maintained parenchymal distribution, whereas Yap had nuclear localizations that spread from periportal to central parenchyma (Figure 3D,E). Particularly, *Ctgf* was located in Hnf4 α + periportal areas that were negative for the pericentral hepatocyte marker GS in the PH-treated livers (Figure 3D,F).

3.3 | Hnf4 α knockdown enhances *Ctgf* expression and sustains fibrogenic responses after liver injury

Hepatocyte nuclear factor (Hnf)4 α is essential for termination of liver regeneration while loss of it is associated with hepatocyte proliferation and activation of Tgf- β signaling during liver injury.²⁸ To determine whether Hnf4 α regulates *Ctgf* during ethanol/ CCl_4 induced liver injury, we screened four siRNAs in piLentiviral vector and identified siHnf4 α #3 with target murine sequences at 833-861bp (NM_008261.2) that caused more than 85% downregulation of Hnf4 α expression in Hepal-6 hepatoma cells (Figure 4A,B) and 75%-85% in mouse livers (Figure 4C,D). Several Hnf4 α target genes, which encode sodium taurocholate cotransporting polypeptide (Slc10a1),²⁹ UDP glucuronosyltransferase 2 family polypeptide B1 (Ugt2b1),³⁰ and Cytochrome P450 member 7a1 (CYP7a1),³¹ were lower in the mouse livers that carried lentivirus expressing siHnf4 α #3 than those containing scramble siRNA during ethanol/ CCl_4 -induced liver injury (Supplementary Figure 4). This siRNA-mediated Hnf4 α knockdown was also associated with enhanced expression of *Ctgf*, in addition to upregulation of α SMA and Collagen type I (Figure 4C,D). IHC and Sirius Red staining verified increased areas of α SMA positive cell population and elevated collagen deposition, respectively (Figure 4E).

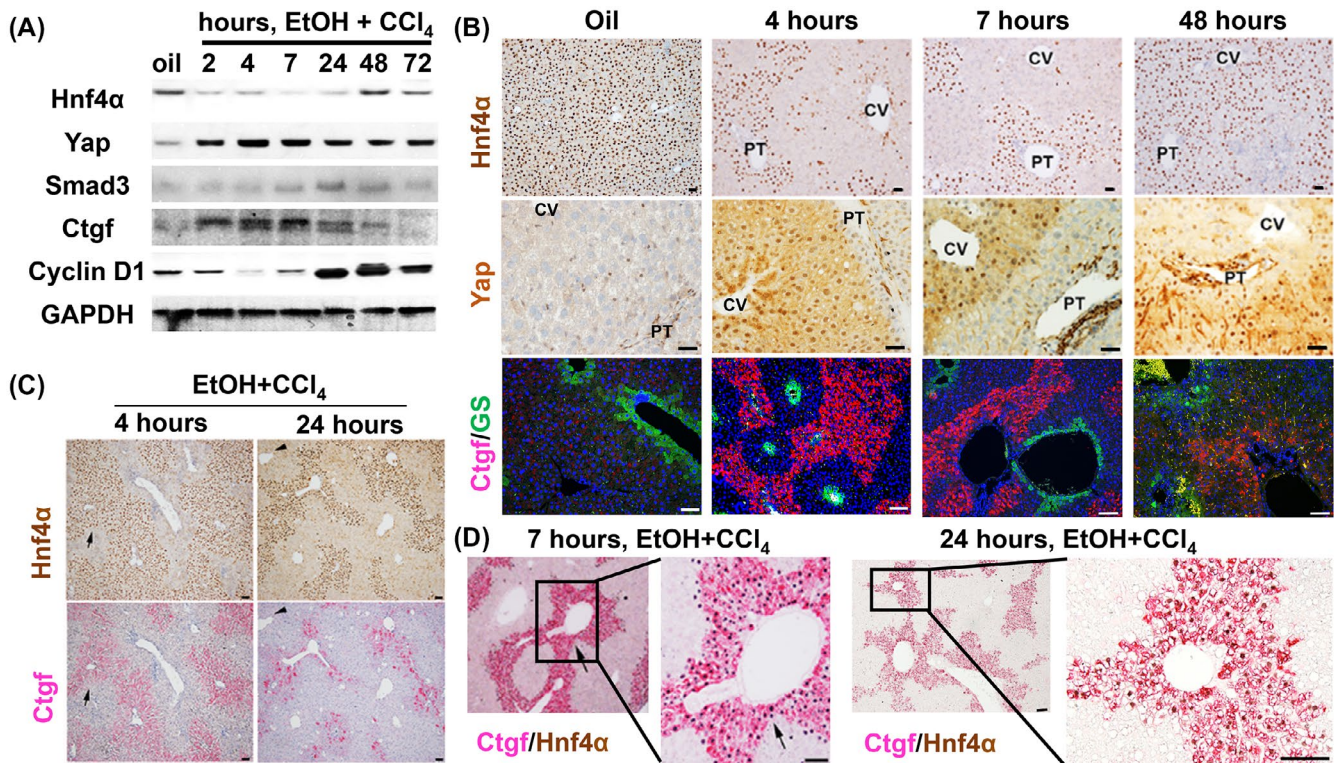


FIGURE 2 *Ctgf* upregulation is associated with loss of *Hnf4α* as well as activation of *Yap* and *Smad3* after EtOH/ CCl_4 -induced liver injury. A, Western blotting determined expression patterns of tested genes in mouse livers after EtOH-fed/ CCl_4 co-treatment. B, IHC labeled *Hnf4α*, *Yap*, *Ctgf* and *GS* on EtOH-fed livers that received oil or CCl_4 administration. C and D, Dual staining showed periportal co-localization of *Ctgf* and *Hnf4α* protein after liver injury. Arrows indicate the same periportal areas in each set of images. Scale bar: 100 μm

To test whether *Hnf4α* knockdown in mouse hepatocytes influenced hepatic stellate cell activation *in vitro*, we first examined the effects of *siHnf4α#3* on *Ctgf* production in AML12 cells in absence or presence of Tgf- β 1 stimulation. Lentivirus expressing *siHnf4α#3* gave rise to very low levels of *Hnf4α* protein, but did not affect *Ctgf* production in AML12 hepatocytes without Tgf- β 1 treatment (left panel, Supplementary Figure 5A). This could be due to low basal levels of *Ctgf* expression in normal hepatocytes. In contrast, stimulation by recombinant murine Tgf- β 1 protein (2 ng/mL) significantly upregulated *Ctgf* in AML12 cells that were transduced with *siHnf4α#3* lentivirus compared to scramble controls (right panel, Supplementary Figure 5A). These results implicated that loss of *Hnf4α* enhanced *Ctgf* induction by Tgf- β 1 in mouse hepatocytes. Then we used conditioned media from the Tgf- β 1-stimulated AML12 cells and treated LX-2 human stellate cells. The qRT-PCR analyses detected higher levels of *α SMA* and *Collagen 1* transcripts in LX-2 cells that were exposed to conditioned media from AML12 cells carrying *siHnf4α#3* than those of scramble controls (Supplementary Figure 5B). These data were in agreement with our *in vivo* results that *Hnf4α* knockdown increased *Ctgf* expression and liver fibrogenesis after ethanol/ CCl_4 -induced liver injury in Figure 4.

3.4 | The CTGF promoter contains an *Hnf4α* binding site that overlaps with cis-elements for *Yap*

The human *CTGF* promoter contains consensus sequences for Tgf- β , *Smad3*, and *Yap/TEAD*.^{32,33} Our computational annotation identified DNA sequence “GTCAAGGGGTCAGG” that resembles a variant direct repeat (DR) 2 for *Hnf4α* binding in both human and mouse promoters of the *CTGF* gene. As shown in Figure 5A, these putative *Hnf4α* binding sequences overlap with a known Tgf- β regulatory element downstream of *cis*-elements for *Yap/TEAD* and *Smad3*.^{8,32,33} Next, we generated plasmids expressing individual Myc tagged murine *Hnf4α*, *Yap* and *Smad3* (*Hnf4α*:Myc, *Yap*:Myc, and *Smad3*:Myc) in Supplementary Figure 6A. PCR-based ChIP assays verified association of the *CTGF* promoter with *Hnf4α*:Myc, *Yap*:Myc, and *Smad3*:Myc proteins (Figure 5B). SEAP assays showed that the *Hnf4α*:Myc protein induced 1.91-fold increase of wild-type *CTGF* promoter than empty vector in HEK293 cells, whereas a mutant promoter that did not have this binding site lost the *Hnf4α*-induced activity (Figure 5C). Direct evidence about *Hnf4α* binding to the *CTGF* promoter was detected as shift bands in gel shift assays. In addition, the DNA/*Hnf4α* complexes

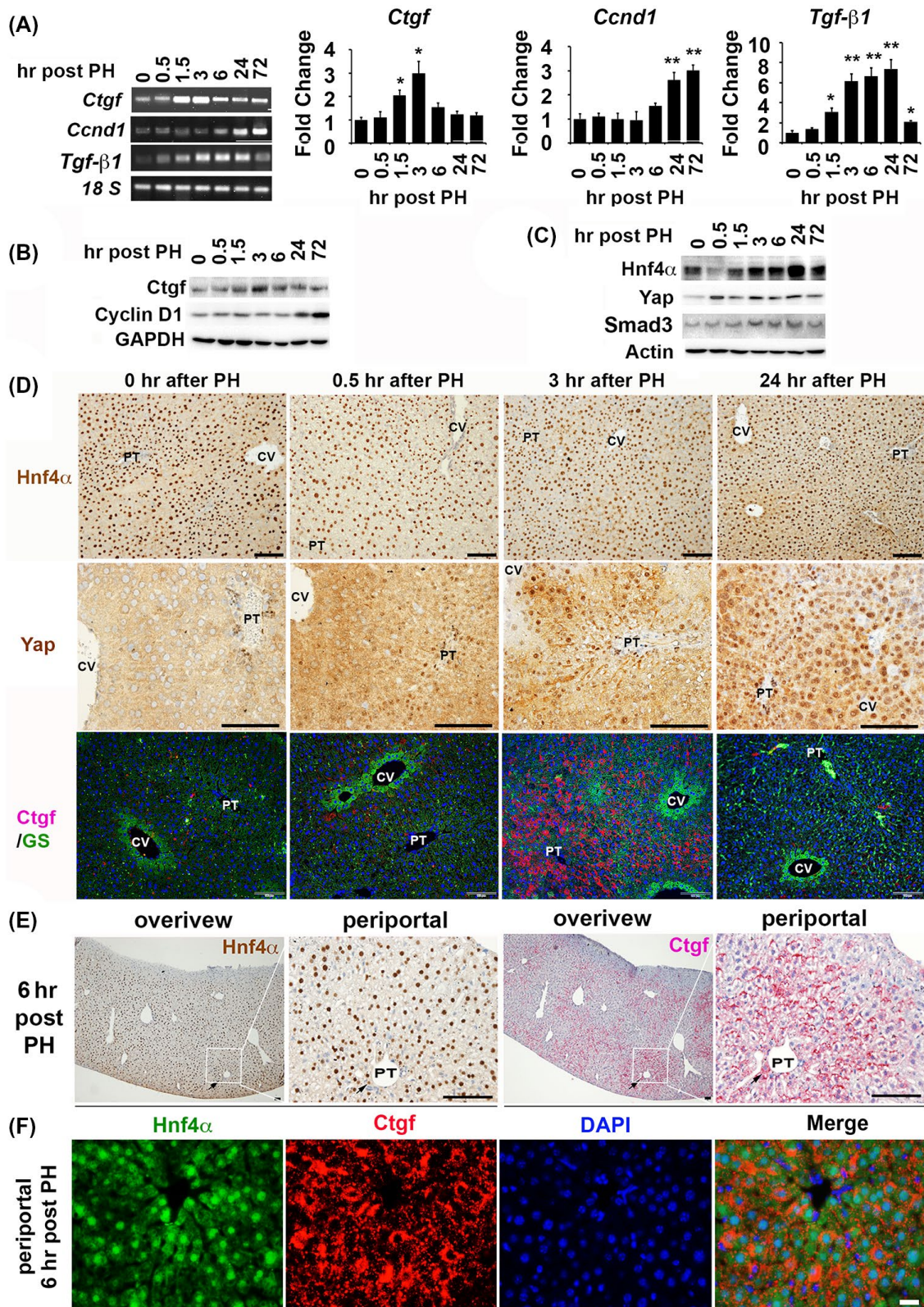


FIGURE 3 *Ctgf* upregulation is associated with transient decline of Hnf4 α during early stage of liver regeneration following PH. *Ctgf* and key regulators for transcriptional reprogramming were examined by qRT-PCR analysis (A) and Western blotting (B and C) in PH-treated livers. Results in (A) were means \pm SEM (n = 5 per group). * $P < .05$ and ** $P < .005$ relative to tested genes of control group (0 hr). (D) IHC labeled Hnf4 α , Yap, Ctgf, and the pericentral hepatocyte marker GS on PH treated livers. (E) Two sets of images are low and high magnifications of consecutive sections showing Ctgf in Hnf4 α ⁺ periportal hepatocytes. (F) The immunofluorescent staining confirmed Ctgf localization in Hnf4 α ⁺ periportal areas. Image were taken in the same areas for Ctgf (red) and Hnf4 α (green). DAPI was stained for nucleus. Scale bar: 100 μ m. hr, hour; PT, portal tract; CV, central vein

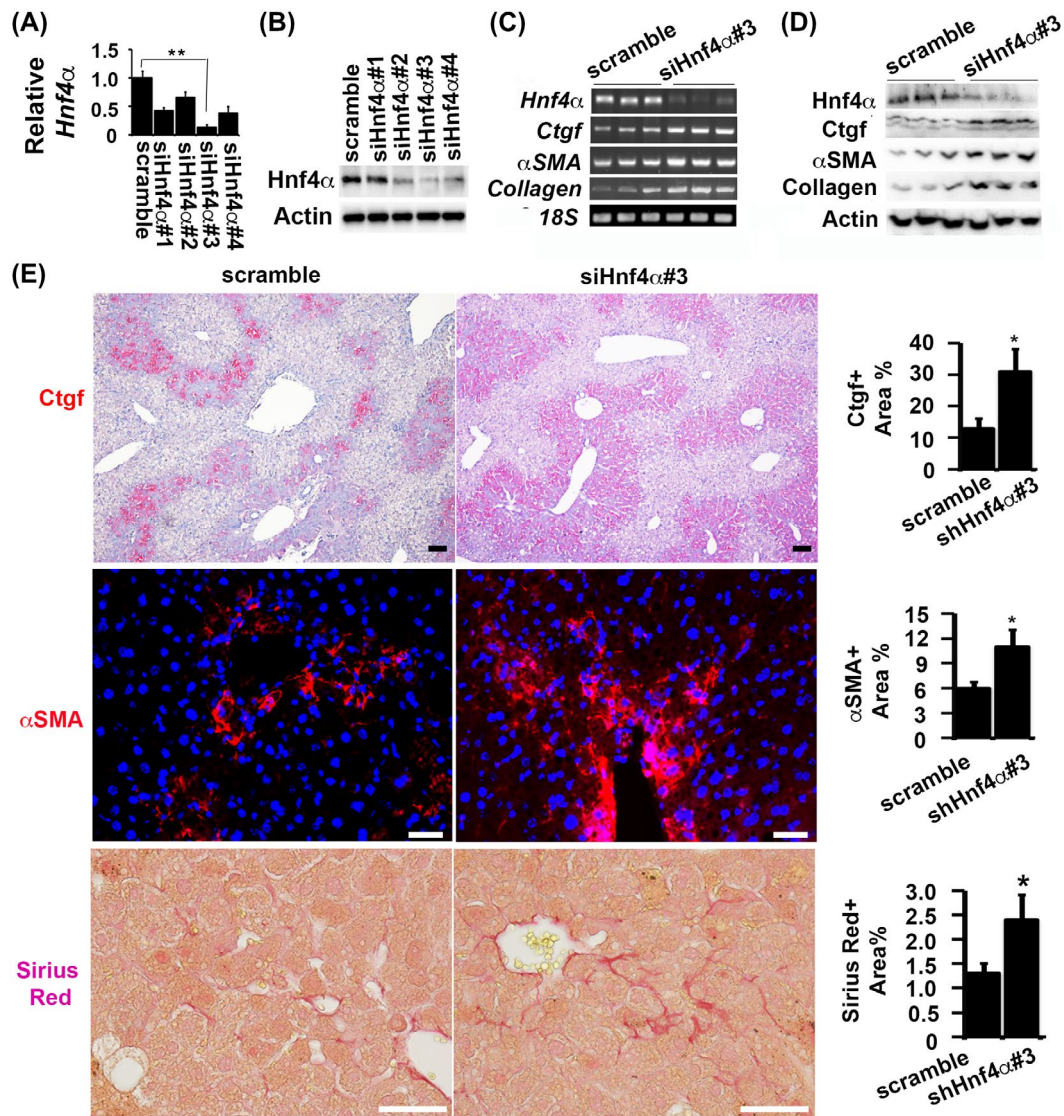


FIGURE 4 Hnf4α knockdown enhances *Ctgf* upregulation and liver fibrogenesis after ethanol/CCl₄ treatment. A and B, Out of four *Hnf4α* siRNAs (*siHnf4α*), #3 in piLentivirus vector had the highest efficiency to inhibit *Hnf4α* mRNA (A) and protein (B) in Hep1-6 cells. Values in (A) were average ± SD from triplicated experiments. **P* < .05 and ***P* < .005 relative to scramble controls. C-E, *Hnf4α* knockdown in ethanol/CCl₄ treated livers carrying piLentivirus-*siHnf4α*#3 caused increased expression of *Ctgf*, *αSMA*, and *Collagen type I* genes as determined by RT-PCR (C), Western blotting (D), and IHC (E). Stained areas were quantified based on image analysis of at least 10 random fields (200× magnification). Data were expressed as means ± SEM (n = 3 animals per group). **P* < .05 (Student's *t* test)

could be disturbed with excessive cold wild-type probe or a mutant probe (Figure 5D). Furthermore, this binding was specific since addition of Hnf4α antibody or in combination with Myc antibody could form “super-shifted” products with higher molecular weight (Figure 5D).

3.5 | Hnf4α mediates fine-tuned regulation of *Ctgf* via antagonistic effects on Yap activity in vitro

Yap and Hnf4α can reciprocally repress each other in regulating gene expression, whereas Yap and Tgf-β are co-operative

partners with synergistic effects on *Ctgf* expression.^{4,33,34} Hnf4α can directly interact with Yap/TEAD complexes and antagonize their activities leading to *ctgf* downregulation.³⁴ In an effort to clarify regulatory mechanisms of *Ctgf* expression in vitro, we first downregulated HNF4α in HepG2 cells and tested its effects on Yap, Tgf-β, and Smad3 activities. Significant knockdown was achieved with 50 nM siHNF4α that targeted 1017-1041 bp of this gene (Supplementary Figure 6B). In comparison to scramble siRNA control, this *siHNF4α* treatment increased *CTGF* promoter activities after co-stimulation by Tgf-β1 protein (5 ng/mL), or co-transfection with Myc tagged plasmids for Yap, Smad3, or in combination (Figure 5E). Conversely, when we expressed the *Hnf4α*:Myc plasmid

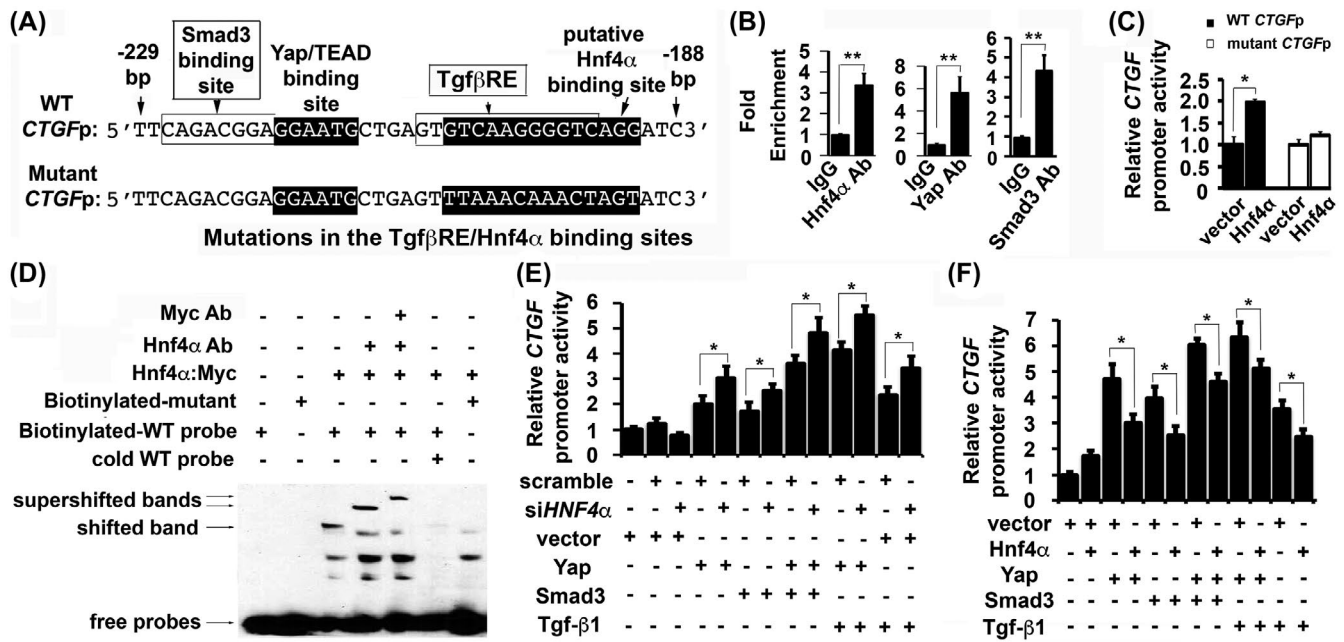


FIGURE 5 Hnf4 α binds to *CTGF* promoter and exhibits antagonistic effects on Yap and Tgf- β /Smad3 activities in vitro. A, A diagram shows cis-elements in wild-type human *CTGF* promoter (WT-*CTGFp*) and mutant *CTGFp*. B, Myc-tagged regulators were expressed in HEK293 cells and their binding to WT-*CTGFp* was verified in ChIP assays. Fold enrichment data were expressed as means \pm SEM from triplicated experiments. $^{***}P < .005$ (Student's *t* test). C, Hnf4 α activated WT-*CTGFp* but not mutant *CTGFp* in HEK293 cells. D, Gel shift assays detected specific complexes of Hnf4 α :Myc with a biotinylated WT probe, which could form super-shifted bands with Hnf4 α antibody (Ab) or combined treatment with Myc Ab. Excessive cold WT or labeled mutant probes competed with or disrupted the probe DNA/protein complex formation. E and F, Downregulation of HNF4 α enhanced WT-*CTGFp* activities in HepG2 cells, whereas HEK293 cells that overexpressed Hnf4 α gene exhibited decrease in WT-*CTGFp* activities. Data in (C, E and F) were expressed as means \pm SD from triplicate tests. $^{*}P < .05$ (Student's *t* test)

in HEK293 cells, the activities of *CTGF* promoter that were stimulated by Tgf- β 1, Yap, Smad3, or in combination became significantly lower than control cells that were transfected with empty vector (Figure 5F). These results indicated that Hnf4 α could mediate fine-tuned regulation of the *CTGF* promoter via antagonism of Yap and the Tgf- β /Smad3 activities.

4 | DISCUSSION

Liver regeneration involves extensive cellular changes and coordinated extracellular remodeling. Alterations in extracellular matrix composition take place immediately after injury and guide reparative processes following PH, CCl₄, or other drugs poisoning.^{35,36} Without proper microenvironments, hepatocytes are unable to regenerate in cirrhotic livers.³⁷ Ctgf is a matricellular protein capable of regulating cell motility and mobility through binding to growth factors, receptors, and matrix proteins.⁹ The formation of Ctgf-enriched microenvironments represents a proliferative and profibrogenic mechanism because conditional knockouts showed downregulation of genes in collagen fibril organization, cell adhesion, cell proliferation, and cell migration after ethanol/CCl₄ treatment. Our most recent studies showed that Ctgf is a critical immune-modulator. Endothelial specific *Ctgf*

knockouts exhibit defects in recruitment of CD11b⁺ inflammatory cells.³⁸ CD11b⁺ macrophages are the main cellular source of pro-inflammatory cytokines during PH or CCl₄ induced liver injury.^{38,39} CD11b is encoded by the integrin α M gene and Ctgf is able to bind integrin α M β 2 for monocyte recruitment.⁴⁰ Thus, downregulation of pro-inflammatory genes in damaged *Ctgf* null livers could be explained by low efficiency of recruitment of CD11b⁺ macrophages in the absence of this pro-adhesion molecule.

Hnf4 α is a master regulator for metabolic homeostasis in hepatocytes. Injury-induced stimuli disrupt homeostasis resulting in loss of Hnf4 α protein. This study showed transient loss of Hnf4 α protein in nuclear fractions at 0.5 to 1.5 hours after PH and prolonged loss of this protein for 2-3 days during CCl₄-induced injury in absence or presence of moderate ethanol feeding. Hnf4 α loss after PH should not be due to tissue necrosis since liver injury following surgical resection does not involve cell death and hepatic inflammation. In another model of liver regeneration that involves hepatocyte death after metabolism of carbon tetrachloride in central zones, Hnf4 α loss in nuclei of peri-central hepatocytes took place as early as 2-4 hours post CCl₄ intoxication, whereas necrosis was evident at later stages (24-72 hours) of the liver damages. Although Hnf4 α loss might take place in necrotic tissues, we argued other

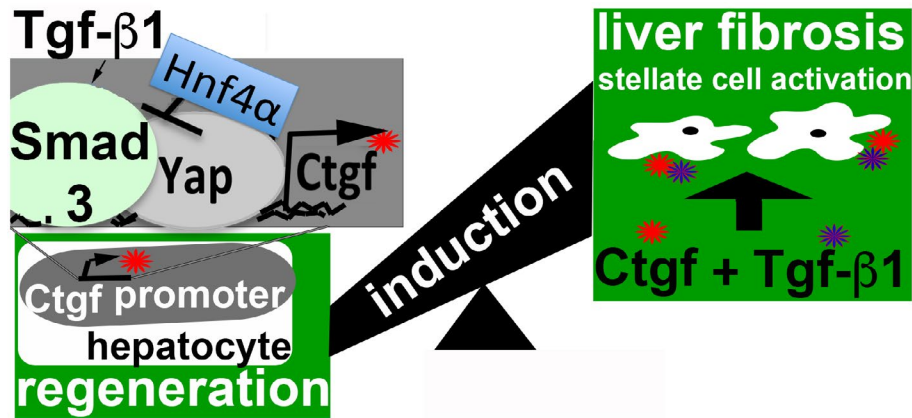


FIGURE 6 A model about *Ctgf* regulation by Hnf4 α , Yap, and Tgf- β /Smad3 signaling during liver regeneration. Hepatocytes exit quiescence after injury and reset transcriptional programs regulated by Hnf4 α and Yap for regeneration. Failure to regenerate causes scarring that overproduces profibrotic factors such as Ctgf and Tgf- β . We propose that *Ctgf* production is a result of transient reprogramming in regenerating livers characterized by Hnf4 α decline in conjunction with activation of Yap and Tgf- β /Smad3 signaling. Hnf4 α antagonism of Yap and Tgf- β /Smad3 activities can downregulate *Ctgf* after the completion of liver regeneration. Otherwise, profibrotic signals are sustained leading to overproduction of Ctgf protein that may potentiate Tgf- β actions and promote hepatic stellate cell activation during liver fibrosis

mechanisms that involve deregulation of this protein for hepatocyte priming during early stages of CCl₄-triggered liver regeneration. In fact, cellular localization and protein levels of nuclear receptors including Hnf4 α can be regulated through post-translation modifications such as acetylation and phosphorylation.^{41,42}

Hnf4 α antagonism of Yap and Tgf- β /Smad3 via *cis*-elements in *Ctgf* promoter represents a potential mechanism to balance liver regeneration and prevent liver fibrosis. A rapid induction of *Ctgf* was observed after PH, which could be due to the transient decline of Hnf4 α . It was reported that Hnf4 α resets transcriptional regulatory networks and represses pro-mitotic genes in hepatocytes within hours after PH.⁴³ More pronounced reprogramming occurred after CCl₄ toxicity according to sustained loss of Hnf4 α . Furthermore, moderate ethanol pre-exposure potentiated this CCl₄-triggered reprogramming due to the prolonged loss of Hnf4 α , increased nuclear accumulation of Yap, and elevated expression of Ctgf and fibrosis related genes. As shown in Figure 6, we proposed a model about *Ctgf* upregulation during liver regeneration that involved transcriptional regulation mediated by Hnf4 α , Yap and Tgf- β /Smad3 signaling. We speculated that knocking down of *Hnf4 α* decreased the antagonistic control of Yap and Tgf- β /Smad3, thereby leading to enhanced hepatocyte proliferation, increased *Ctgf*, and strong fibrogenic response in *Hnf4 α* -downregulated livers after ethanol/CCl₄-induced injury. Taking into account the fact that Hnf4 α loss in conjunction with activation of Yap and the Tgf- β /Smad3 signaling occurs in many liver diseases, it is conceivable that similar mechanisms of transcriptional reprogramming occurs and induces high level of *Ctgf* that contributes to the development of liver fibrosis and HCC in these pathological

conditions. Recently, it was reported that the process of gene expression from its genomic form is completely different with that from the cDNA form, regarding epigenetic modification, protein-DNA interaction, etc.^{44,45} Thus, the crosstalk between Ctgf and Hnf4 α in its cellular endogenous manner needs to be extensively explored.

In summary, Ctgf is a key player in liver regeneration and can promote hepatic inflammation, hepatocyte proliferation, and collagen synthesis. Its induction in regenerating hepatocytes after chemically and surgically induced liver regeneration is likely a result of transcriptional reprogramming characterized by Hnf4 α decline in conjunction with activation of Yap and the Tgf- β /Smad3 signaling. Hnf4 α mediates fine-tuned regulation of *Ctgf* expression via a novel *cis*-element to antagonize Yap and Tgf- β /Smad3 activities. Hnf4 α antagonism balances regenerative signaling and prevents overproduction of fibrotic signals. This new mechanism may have therapeutic implication for rationale designs to improve liver regeneration and reduce abnormal repair caused by hepatic insults such as alcohol.

ACKNOWLEDGMENTS

We want to thank Drs. Bryon Petersen, Gregory Schultz, Edward Scott, and Arun Srivastava for helping establishment of mouse models and discussion about this manuscript. This study is supported by National Institutes of Health NIAAA KO1AA024174 and R01AA028035 grants and Children Miracle Research Foundation grant awarded to Dr. L Pi. Dr. Ling is supported by the National Key Research and Development Program of China (2018YFA0109400), the Shanghai Sailing Program (17YF1401300) and Shanghai Eastern Scholarship (TP2016004).

CONFLICT OF INTERESTS

The authors declare that there is no conflict of interest regarding publication of this manuscript.

AUTHOR CONTRIBUTIONS

L. Pi, C. Ling, L. Wu, and C. Qi designed research. L. Pi, and C. Ling established mouse models. J. Zhou, X. Sun, L. Yang, G. Ran, J. Wang, L. Wang, and L. Pi performed research and analyzed data. C. Ling and L. Pi wrote the manuscript. Final approval of the paper was done by all authors.

REFERENCES

- Nwidu LL, Oboma YI. Telfairia occidentalis (Cucurbitaceae) pulp extract mitigates rifampicin-isoniazid-induced hepatotoxicity in an in vivo rat model of oxidative stress. *J Integr Med.* 2019;17:46-56.
- Fausto N, Campbell JS, Riehle KJ. Liver regeneration. *J Hepatol.* 2012;57:692-694.
- Ling CQ, Fan J, Lin HS, et al. Clinical practice guidelines for the treatment of primary liver cancer with integrative traditional Chinese and Western medicine. *J Integr Med.* 2018;16:236-248.
- Oh SH, Swiderska-Syn M, Jewell ML, Premont RT, Diehl AM. Liver regeneration requires Yap1-TGFbeta-dependent epithelial-mesenchymal transition in hepatocytes. *J Hepatol.* 2018;69:359-367.
- Huck I, Gunewardena S, Espanol-Suner R, Willenbring H, Apte U. Hepatocyte nuclear factor 4 alpha activation is essential for termination of liver regeneration in mice. *Hepatology.* 2019;70:666-681.
- Patel SH, Camargo FD, Yimlamai D. Hippo signaling in the liver regulates organ size, cell fate, and carcinogenesis. *Gastroenterology.* 2017;152:533-545.
- Urtasun R, Latasa MU, Demartis MI, et al. Connective tissue growth factor autocriny in human hepatocellular carcinoma: oncogenic role and regulation by epidermal growth factor receptor/yes-associated protein-mediated activation. *Hepatology.* 2011;54:2149-2158.
- Zhao B, Ye X, Yu J, et al. TEAD mediates YAP-dependent gene induction and growth control. *Genes Dev.* 2008;22:1962-1971.
- Gressner OA, Gressner AM. Connective tissue growth factor: a fibrogenic master switch in fibrotic liver diseases. *Liver Int.* 2008;28:1065-1079.
- Abreu JG, Ketpura NI, Reversade B, De Robertis EM. Connective-tissue growth factor (CTGF) modulates cell signalling by BMP and TGF-beta. *Nat Cell Biol.* 2002;4:599-604.
- Tong Z, Chen R, Alt DS, Kemper S, Perbal B, Brigstock DR. Susceptibility to liver fibrosis in mice expressing a connective tissue growth factor transgene in hepatocytes. *Hepatology.* 2009;50:939-947.
- Kuttippurathu L, Juskeviciute E, Dippold RP, Hoek JB, Vadigepalli R. A novel comparative pattern analysis approach identifies chronic alcohol mediated dysregulation of transcriptomic dynamics during liver regeneration. *BMC Genom.* 2016;17:260.
- Su AI, Guidotti LG, Pezacki JP, Chisari FV, Schultz PG. Gene expression during the priming phase of liver regeneration after partial hepatectomy in mice. *Proc Natl Acad Sci USA.* 2002;99:11181-11186.
- Pi L, Robinson PM, Jorgensen M, et al. Connective tissue growth factor and integrin alphavbeta6: a new pair of regulators critical for ductular reaction and biliary fibrosis in mice. *Hepatology.* 2015;61:678-691.
- Pi L, Fu C, Lu Y, et al. Vascular endothelial cell-specific connective tissue growth factor (CTGF) is necessary for development of chronic hypoxia-induced pulmonary hypertension. *Front Physiol.* 2018;9:138.
- Liu S, Shi-wen X, Abraham DJ, Leask A. CCN2 is required for bleomycin-induced skin fibrosis in mice. *Arthritis Rheum.* 2011;63:239-246.
- Pi L, Oh SH, Shupe T, Petersen BE. Role of connective tissue growth factor in oval cell response during liver regeneration after 2-AAF/PHx in rats. *Gastroenterology.* 2005;128:2077-2088.
- Roychowdhury S, Chiang DJ, Mandal P, et al. Inhibition of apoptosis protects mice from ethanol-mediated acceleration of early markers of CCl4 -induced fibrosis but not steatosis or inflammation. *Alcohol Clin Exp Res.* 2012;36:1139-1147.
- Pi L, Shenoy AK, Liu J, et al. CCN2/CTGF regulates neovessel formation via targeting structurally conserved cysteine knot motifs in multiple angiogenic regulators. *FASEB J.* 2012;26:3365-3379.
- Lin S, Liu Q, Lelyveld VS, Choe J, Szostak JW, Gregory RI. Mettl1/Wdr4-mediated m(7)G tRNA methylome is required for normal mRNA translation and embryonic stem cell self-renewal and differentiation. *Mol Cell.* 2018;71(244-255):e245.
- Dobin A, Davis CA, Schlesinger F, et al. STAR: ultrafast universal RNA-seq aligner. *Bioinformatics.* 2013;29:15-21.
- Anders S, Pyl PT, Huber W. HTSeq—a Python framework to work with high-throughput sequencing data. *Bioinformatics.* 2015;31:166-169.
- Robinson MD, McCarthy DJ, Smyth GK. edgeR: a Bioconductor package for differential expression analysis of digital gene expression data. *Bioinformatics.* 2010;26:139-140.
- da Huang W, Sherman BT, Lempicki RA. Systematic and integrative analysis of large gene lists using DAVID bioinformatics resources. *Nat Protoc.* 2009;4:44-57.
- Varghese F, Bukhari AB, Malhotra R, De A. IHC Profiler: an open source plugin for the quantitative evaluation and automated scoring of immunohistochemistry images of human tissue samples. *PLoS ONE.* 2014;9:e96801.
- Wu Y, Xie L, Wang M, et al. Mettl3-mediated m(6)A RNA methylation regulates the fate of bone marrow mesenchymal stem cells and osteoporosis. *Nat Commun.* 2018;9:4772.
- Leask A, Sa S, Holmes A, Shiwen X, Black CM, Abraham DJ. The control of ccn2 (ctgf) gene expression in normal and scleroderma fibroblasts. *Mol Pathol.* 2001;54:180-183.
- Deshpande KT, Liu S, McCracken JM, et al. Moderate (2%, v/v) ethanol feeding alters hepatic wound healing after acute carbon tetrachloride exposure in mice. *Biomolecules.* 2016;6:5.
- Geier A, Martin IV, Dietrich CG, et al. Hepatocyte nuclear factor-4alpha is a central transactivator of the mouse Ntcp gene. *Am J Physiol Gastrointest Liver Physiol.* 2008;295:G226-G233.
- Lu H, Gonzalez FJ, Klaassen C. Alterations in hepatic mRNA expression of phase II enzymes and xenobiotic transporters after targeted disruption of hepatocyte nuclear factor 4 alpha. *Toxicol Sci.* 2010;118:380-390.
- Stroup D, Chiang JY. HNF4 and COUP-TFII interact to modulate transcription of the cholesterol 7alpha-hydroxylase gene (CYP7A1). *J Lipid Res.* 2000;41:1-11.
- Grotendorst GR, Okochi H, Hayashi N. A novel transforming growth factor beta response element controls the expression of the connective tissue growth factor gene. *Cell Growth Differ.* 1996;7:469-480.

33. Fujii M, Toyoda T, Nakanishi H, et al. TGF-beta synergizes with defects in the Hippo pathway to stimulate human malignant mesothelioma growth. *J Exp Med*. 2012;209:479-494.
34. Cai WY, Lin LY, Hao H, et al. Yes-associated protein/TEA domain family member and hepatocyte nuclear factor 4-alpha (HNF4alpha) repress reciprocally to regulate hepatocarcinogenesis in rats and mice. *Hepatology*. 2017;65:1206-1221.
35. Klaas M, Kangur T, Viil J, et al. The alterations in the extracellular matrix composition guide the repair of damaged liver tissue. *Sci Rep*. 2016;6:27398.
36. Nwido LL, Teme RE. Hot aqueous leaf extract of *Lasianthera africana* (Icacinaeae) attenuates rifampicin-isoniazid-induced hepatotoxicity. *J Integr Med*. 2018;16:263-272.
37. Liu L, Yannam GR, Nishikawa T, et al. The microenvironment in hepatocyte regeneration and function in rats with advanced cirrhosis. *Hepatology*. 2012;55:1529-1539.
38. Sato A, Nakashima H, Nakashima M, et al. Involvement of the TNF and FasL produced by CD11b Kupffer cells/macrophages in CCl4-induced acute hepatic injury. *PLoS ONE*. 2014;9:e92515.
39. Nishiyama K, Nakashima H, Ikarashi M, et al. Mouse CD11b+kupffer cells recruited from bone marrow accelerate liver regeneration after partial hepatectomy. *PLoS ONE*. 2015;10:e0136774.
40. Schober JM, Chen N, Grzeszkiewicz TM, et al. Identification of integrin alpha(M)beta(2) as an adhesion receptor on peripheral blood monocytes for Cyr61 (CCN1) and connective tissue growth factor (CCN2): immediate-early gene products expressed in atherosclerotic lesions. *Blood*. 2002;99:4457-4465.
41. Soutoglou E, Katrakili N, Talianidis I. Acetylation regulates transcription factor activity at multiple levels. *Mol Cell*. 2000;5:745-751.
42. Sun K, Montana V, Chellappa K, et al. Phosphorylation of a conserved serine in the deoxyribonucleic acid binding domain of nuclear receptors alters intracellular localization. *Mol Endocrinol*. 2007;21:1297-1311.
43. Jiao H, Zhu Y, Lu S, Zheng Y, Chen H. An integrated approach for the identification of HNF4alpha-centered transcriptional regulatory networks during early liver regeneration. *Cell Physiol Biochem*. 2015;36:2317-2326.
44. Zheng M, Mitra RN, Filonov NA, Han Z. Nanoparticle-mediated rhodopsin cDNA but not intron-containing DNA delivery causes transgene silencing in a rhodopsin knockout model. *FASEB J*. 2016;30:1076-1086.
45. Mitra RN, Zheng M, Weiss ER, Han Z. Genomic form of rhodopsin DNA nanoparticles rescued autosomal dominant Retinitis pigmentosa in the P23H knock-in mouse model. *Biomaterials*. 2018;157:26-39.

SUPPORTING INFORMATION

Additional supporting information may be found online in the Supporting Information section.

How to cite this article: Zhou J, Sun X, Yang L, et al. Hepatocyte nuclear factor 4 α negatively regulates connective tissue growth factor during liver regeneration. *The FASEB Journal*. 2020;34:4970–4983. <https://doi.org/10.1096/fj.201902382R>